Mixing of a Row of Jets with a Confined Crossflow

J. D. Holdeman*
NASA Lewis Research Center, Cleveland, Ohio
and
R. E. Walker†
Aerojet Liquid Rocket Co., Sacramento, Calif.

An empirical model has been developed for predicting the temperature distribution downstream of a row of cool jets injected normal to a hot confined crossflow. The model is based on the assumption that all properly nondimensionalized vertical temperature profiles can be expressed in a self-similar form. The scaling parameters in this form have been correlated in terms of the independent flow and geometric variables. The effect of parametric variation of each of the independent variables on the experimental and predicted profiles are examined. The predicted distributions show excellent agreement with the data over a wide range of the independent variables.

Nomenclature

A_j/A_∞ = orifice area to mainstream area ratio = $(\pi/4)/[(H/D)(S/D)]$
C_d = orifice discharge coefficient
D = orifice diameter; (Fig. 1)
D_j = jet diameter = $D\sqrt{C_d}$
H = duct height = 10.16 cm; (Fig. 1)
J = momentum flux ratio, = $(\rho_j V_j^2)/(\rho_\infty U_\infty^2)$
S = spacing between centerlines of adjacent orifices; (Fig. 1)
T = temperature at any location in flowfield
T_j = jet total temperature
T_∞ = mainstream total temperature, = 600 K
U_∞ = mainstream velocity, = 15 m/sec
V_j = jet velocity
w_j/w_∞ = jet-to-mainstream mass flow ratio; [Eq. (1)]
X = distance downstream from jet injection location; (Fig. 1)
Y = distance above injection plane; (Fig. 1)
Z = off-centerplane distance; (Fig. 1)
θ = dimensionless temperature difference ratio; [Eq. (2)]
ρ_j = jet density
ρ_∞ = mainstream density
σ = standard deviation of data from correlation equations; (Table 1)

Introduction

THE objective of this study was to model the penetration and mixing characteristics of multiple jets of cooling air injected normally into a heated crossflow in a constant area duct. The study was motivated by considerations of dilution zone mixing in gas turbine combustion chambers. For this application, rapid mixing of the diluent air with hot combustion gases leaving the primary zone is desired to 1) provide a rapid quench for any continuing chemical reactions, 2) provide a suitable temperature distribution at the turbine inlet, and 3) reduce combustor length.

The experimental results on which the model is based have been reported by Holdeman, Walker, and Kors,[1] and by Walker and Kors.[2] The temperature field model was developed by Walker and Eberhardt.[3] Data for selected tests from the Ref. 2 experiments have been used by Cox[4] to generate correlations to characterize the dilution process. The results of Refs. 3 and 4 both provide satisfactory profile predictions. In this paper, the effect of parametric variation of each of the independent variables on both the experimental and predicted profiles (using the correlations of Ref. 3) are examined.

The Data Base

A schematic of the multiple jet flowfield with the principal flow and geometric variables identified appears in Fig. 1. The test section was 30.48 cm wide by 10.16 cm high. For all of the test results shown in this paper the nominal mainstream conditions were: velocity, $U_\infty = 15$ m/sec; temperature, $T_\infty = 600$ K. The jet velocity, V_j, was varied from 25 to 85 m/sec with the jets at ambient temperature. The jets entered the test section through sharp-edged orifices in the plate separating the main duct from the secondary air plenum chamber.

The test conditions were established with the jet-to-mainstream momentum flux ratio, $J = (\rho_j V_j^2)/(\rho_\infty U_\infty)$, and the jet-to-mainstream density ratio, ρ_j/ρ_∞, as the primary independent flow variables. Momentum flux ratios investigated ranged from 6 to 60, with density ratios varied from 1.6 to 2.8.

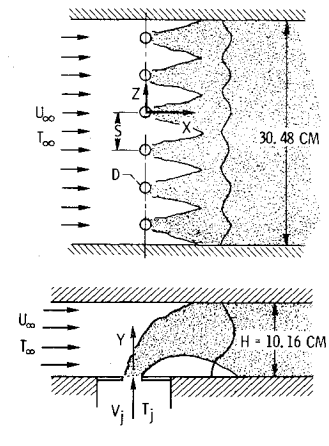

Fig. 1 Schematic of multiple jet flow.

Received Jan. 13, 1976; presented as Paper 76-48 at the AIAA 14th Aerospace Sciences Meeting, Jan. 26-28, 1976; revision received Oct. 1, 1976.
Index category: Jets, Wakes, and Viscid-Inviscid Flow Interactions.
*Aerospace Engineer, Combustion and Pollution Research Branch. Member AIAA.
†Senior Engineer, Analytical Design. Member AIAA.

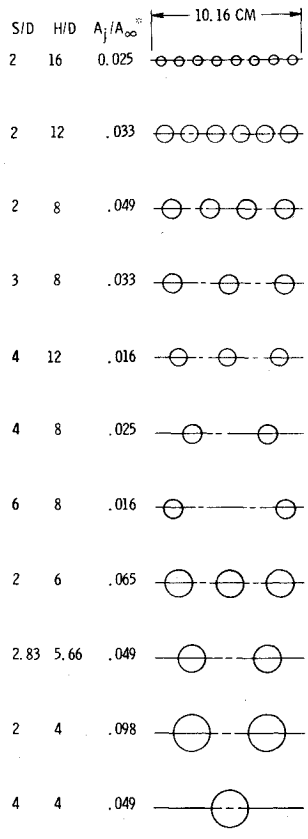

Fig. 2 Orifice plate configurations; $A_j/A_\infty = (\pi/4)/(H/D)/(S/D)$.

The primary independent geometric variables were the orifice size and spacing between adjacent orifices. These were expressed in dimensionless form as the ratio of the duct height to the orifice diameter, $(4 \le H/D \le 16)$, and the ratio of the orifice spacing to the orifice diameter, $(2 \le S/D \le 6)$. Although the experiments were performed with S/D and H/D as the independent geometric variables, the ratio of these, S/H, may be considered as an independent variable in the place of either S/D or H/D. The orifice area may be expressed in dimensionless form as $A_j/A_\infty = (\pi/4)/[(H/D)(S/D)]$ which is the orifice-to-mainstream area ratio. The orifice configurations investigated are shown in Fig. 2.

The ratio of the jet flow to mainstream flow, $\dot{w}_j/\dot{w}_\infty$, is an important variable in combustor design, and can be expressed in terms of the independent flow and geometric variables as

$$\frac{\dot{w}_j}{\dot{w}_\infty} = \left[\sqrt{\frac{\rho_j}{\rho_\infty}}\sqrt{J}\frac{\pi}{4}C_d\right] \Big/ \left[\left(\frac{H}{D}\right)\left(\frac{S}{D}\right)\right] \tag{1}$$

For this investigation, the orifice discharge coefficient, C_d, varied from 0.66 at the lowest momentum flux ratio to 0.62 at the highest momentum flux ratio.

Because the objective of the study was to identify orifice configurations appropriate for optimum mixing within a minimum combustor length, the downstream stations surveyed were defined in terms of the duct height, H. Measurements of total pressure and temperature were made at 20 vertical and 21 horizontal positions in each of five planes at downstream locations from $X/H = 0.25$ to $X/H = 2.0$. The total span of the 21 horizontal positions was varied to correspond to twice the orifice spacing for each plate. This distance varied from 2.54 cm for the smallest orifice spacing to 20.32 cm for the largest spacing. The Z plane through the orifice center is defined as the centerplane ($Z=0$), and the Z plane midway between adjacent orifices is defined as the midplane ($Z=S/2$). Thus the span of the measurements provided 4-fold data redundancy. Additional aspects of the experimental program and the facility used are discussed in Ref. 2.

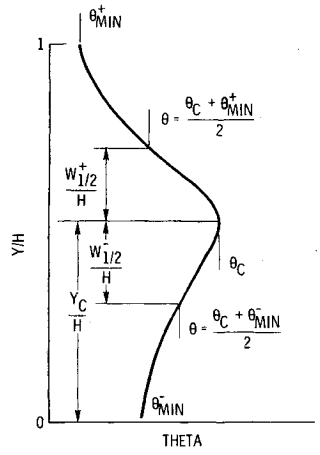

Fig. 3 Schematic of typical vertical temperature profile showing scaling parameters.

The results for the temperature field are presented as vertical profiles of the dimensionless temperature difference ratio θ where

$$\theta = \frac{T_\infty - T}{T_\infty - T_j} \tag{2}$$

and T is the local total temperature, T_∞ is the total temperature of the undisturbed mainstream flow, and T_j is the jet total temperature. Because $T_\infty > T_j$, the largest values of θ in any profile correspond to the coolest regions of the flow.

Flowfield Model

The empirical model for this three-dimensional shear flow is based on the observation that the properly nondimensionalized vertical temperature profiles everywhere in the flowfield can be expressed in the following self-similar form

$$\frac{\theta - \theta^{\pm}_{\min}}{\theta_c - \theta^{\pm}_{\min}} = \exp\left[-\ell n\, 2\left(\frac{\frac{Y}{H} - \frac{Y_c}{H}}{\frac{W^{\pm}_{1/2}}{H}}\right)^2\right] \tag{3}$$

In this expression, θ is the local temperature difference ratio given by Eq. (2), and θ_c, $\theta^{\pm}_{\min}$, Y_c/H, and $W^{\pm}_{1/2}/H$ are scaling parameters as shown in Fig. 3. θ_c is the maximum temperature difference ratio in the vertical profile, and Y_c is its location. The line defined by the locus of Y_c as a function of downstream distance (X) for $Z=0$ is the thermal trajectory (centerline).

Because the flow is confined, and the profiles are not symmetric about the centerline, the half-widths ($W^{\pm}_{1/2}$) and the minimum temperature difference ratios ($\theta^{\pm}_{\min}$) are different for the + side ($Y/H > Y_c/H$) and the − side ($Y/H < Y_c/H$) of the profiles. Correlations have been developed for each of the scaling parameters in terms of the independent variables J, S/D, H/D, X/H, and Z/S. The complete set of correlations are given in the Appendix. This is only one possible set of correlations; Cox[4] gives another set which also yield satisfactory profile predictions. The primary differences between the results given here and those in Ref. 4 are: 1) the forms of the present correlations are simpler than those of Ref. 4, and the relative importance of each of the independent variables is more readily apparent, and 2) profiles can be predicted using the correlations in the Appendix over a wider range of the independent variables since the data base used in the present investigation was larger than the one used in Ref. 4. The main weakness of the present correlations is that their form precludes their use in predicting profiles for semiconfined flows (large H/D or large S/D) or the single jet flow (large H/D and S/D).

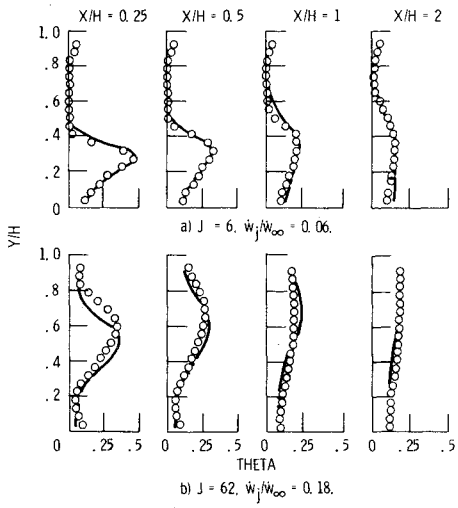

Fig. 4 Variation of centerplane temperature profiles with downstream distance; $S/D=4$, $H/D=8$.

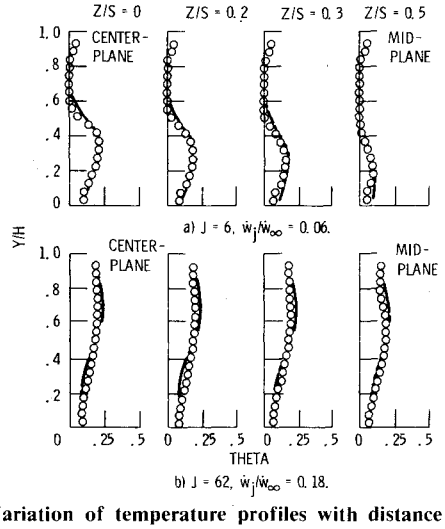

Fig. 5 Variation of temperature profiles with distance from centerplane; $X/H=1$, $S/D=4$, $H/D=8$.

Results and Discussion

Effect of Downstream and Lateral Distance

The variation of the centerplace ($Z=0$) temperature profiles with downstream distance for both the smallest ($J=6$) and largest ($J=60$) momentum flux ratios tested are shown in Fig. 4 for an orifice configuration with $S/D=4$ and $H/D=8$. For this geometry, the agreement between predicted and experimental profiles is slightly better at the low momentum flux ratio than at the high one. At the high momentum flux ratio, the jet penetration increases monotonically with increasing downstream distance. However, at the low momentum flux ratio, the penetration is nonmonotonic, with a slight recurving toward the injection wall evident at the largest downstream distance. This effect appeared whenever the jet penetrated to less than half the duct height, and was particularly acute when a two-dimensional jet flow was established near the injection wall ($Y=0$). In Fig. 5, lateral profiles at $X/H=1$ are shown for the same conditions as in Fig. 4. For the low momentum flux ratio, the profiles vary substantially with lateral distance, and the model provides a satisfactory prediction of both the decrease in the maximum penetration and the decrease in the maximum temperature difference with increasing distance from the centerplane. The isotherm contours ($y-z$ plane) for this condition[2] show the traditional "kidney" shape resulting from the twin vortices which develop with the flow from each

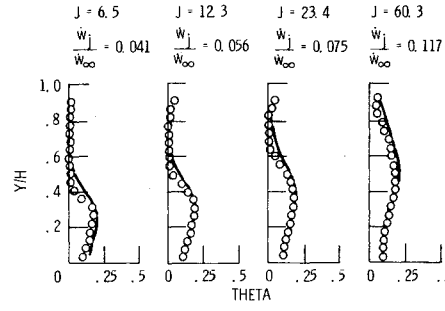

Fig. 6 Effect of momentum flux ratio on centerplane temperature profiles; $X/H=1$, $S/D=4$, $H/D=12$.

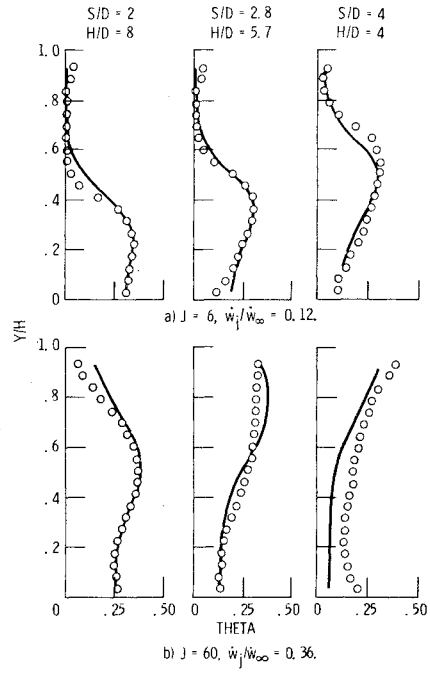

Fig. 7 Effect of geometric variables on centerplane temperature profiles at constant orifice area; $A_j/A_\infty=0.049$, $X/H=1$.

jet. The lateral variation of the temperature profiles is small at the high momentum flux ratio, indicating that there is substantial interaction between adjacent jets, which tends to diffuse the vorticity. The result is a nearly plane flow as shown in Fig. 5b.

Effect of Flow Variables

For each orifice configuration, the penetration of the jets increased as the jet-to-mainstream momentum flux ratio, $J=(\rho_j V_j^2)/(\rho_\infty U_\infty^2)$, increased. The magnitude of this effect is shown by the centerplane ($Z=0$) profiles in Fig. 6. These profiles are at a distance of one duct height downstream from the injection point for a geometry with $S/D=4$ and $H/D=12$. The prediction of the centerplane profiles is good except that the + side half-width is too large for low J values. It should be noted that the ratio of jet flow to mainstream flow increases by approximately a factor of three from $J=6$ to $J=60$, since $\dot{w}_j/\dot{w}_\infty \sim \sqrt{J}$; see Eq. (1).

Although experiments were performed with the density ratio varied from 1.6 to 2.8 at constant momentum flux ratio, no consistent correlation with density ratio was found in the present investigation. Because the range of the density ratio variation was limited, the absence of an explicit density ratio term in the correlations does not imply that the mixing is independent of density ratio for all ρ_j/ρ_∞, but rather indicates that the density ratio effect, if any, is of second-order importance compared to the momentum flux ratio effect. For all comparisons of experimental and predicted profiles in this paper, data for tests with $2.1 \le \rho_j/\rho_\infty \le 2.3$ have been used.

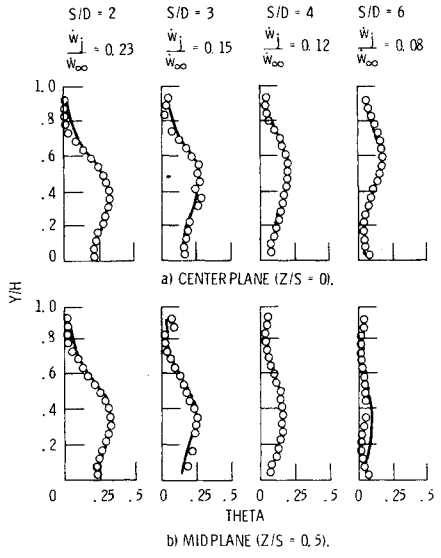

Fig. 8 Effect of varying spacing on temperature profiles for constant orifice diameter; $H/D=8$, $X/H=1$, $J=25$.

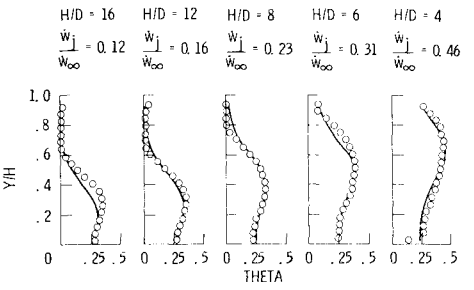

Fig. 9 Effect of varying orifice diameter on centerplane temperature profiles at constant S/D; $S/D=2$, $X/H=1$, $J=25$.

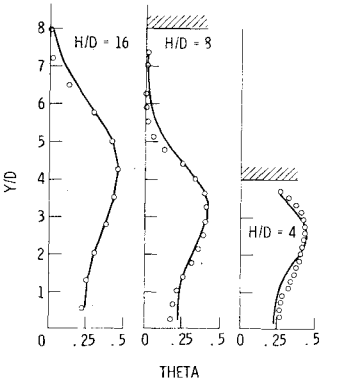

Fig. 10 Effect of confinement by the opposite wall on centerplane temperature profiles at $X/D=4$ for $S/D=2$ and $J=25$.

Effect of Geometric Variables

The momentum flux ratio, and the density ratio are dependent on the combustor design conditions, e.g., inlet temperature and pressure, reference velocity, pressure drop, and fuel-air ratio. Thus for a given combustor, the dilution zone design parameters which may be varied to influence the combustor exit temperature distribution are the orifice diameter, orifice spacing, and orifice shape. However, since the required ratio of jet to mainstream flow for a given combustor can be determined from the design conditions and the desired mean exit temperature, the orifice size and spacing must be correctly coupled to provide the appropriate orifice area. In Fig. 7, centerplane temperature profile data at $X/H=1$ for momentum flux ratios of 6 and 60 are shown for three orifice configurations all having orifice-to-mainstream area ratios of 0.049. The differences in the profiles at each momentum flux ratio indicate that for a given operating condition (constant J and $\dot{w}_j/\dot{w}_\infty$) considerable variations in the downstream temperature distributions can be effected by changes in the orifice diameter and spacing. The most significant difference between the experimental and predicted profiles in Fig. 7 is for the largest orifices at the highest momentum flux ratio. These conditions cause flow impingement on the opposite wall, and the temperature distributions in the resultant strongly bifurcated flow do not conform to the self-similar profile shape assumed in the model. Thus, the lack of agreement between predicted and experimental profiles is not surprising.

The variations shown in Fig. 7 are consistent with the results of Norgren and Humenik,[5] where fewer large orifices were found to provide better jet penetration than a larger number of small orifices for the same orifice area. In the following paragraphs, the effects of parametric variation of the geometric variables at a constant (nominal) momentum flux ratio of $J=25$ are discussed.

Effect of Varying Orifice Spacing at Constant Orifice Diameter ($H/D=8$, $J=25$, $X/H=1$)

For a given jet diameter, momentum flux ratio, and downstream distance the penetration of the dilution jets increases with increasing spacing as shown in the centerplane profiles in Fig. 8a. This occurs because the interference between adjacent jets decreases as spacing increases. Also, the maximum temperature difference in each profile decreases with increased spacing as would be expected since the ratio of jet flow to mainstream flow varies inversely with S/D; see Eq. (1). The agreement between experimental and predicted profiles is excellent in all cases. The variation of the corresponding midplane profiles is shown in Fig. 8b. As spacing increases, the centerplane and midplane profiles differ as the flow develops three-dimensionally. The prediction of the midplane profiles is good, but of course there is some spacing for which further increases would have no effect on the experimental distributions. Beyond this spacing, the flow is semiconfined and the model (as presently formulated) is not appropriate.

Effect of Varying Orifice Diameter at Constant S/D ($S/D=2$, $J=25$)

For a given S/D, momentum flux ratio, and downstream distance, the jet penetration increases significantly with increasing orifice diameter (decreasing H/D) as shown in the centerplane profiles at $X/H=1$ in Fig. 9. Also the maximum temperature difference increases slightly with increasing orifice diameter, but the dominant difference in these profiles is the percentage of the span cooled by the dilution flow. Since these profiles are for constant ρ_j/ρ_∞, J, and S/D, the ratio of jet flow to mainstream flow increases by a factor of 4 from $H/D=16$ to $H/D=4$; see Eq. (1). The predicted and experimental profiles compare favorably except for the smallest orifice size where the model underpredicts the trajectory (too much recurving) and underpredicts the maximum temperature difference.

Some insight into the confining effect of the opposite wall is given by the centerplane profiles of θ vs. Y/D at constant X/D (Fig. 10). The maximum temperature difference decreases slightly with decreasing H/D, but the primary effect is the suppression of the jet penetration (expressed as Y_c/D). The effects shown here are in agreement with the results of experiments on heated jets in a confined crossflow reported by Kamotani and Greber.[6]

Effect of Varying Orifice Diameter at Constant Spacing ($S/H=0.5$, $J=25$)

For a constant S/H (constant spacing), constant momentum flux ratio, and constant downstream distance, increasing the orifice diameter shifts the temperature profiles to higher θ values consistent with the greater dilution airflow. Although the penetration of the jets also increases slightly, the

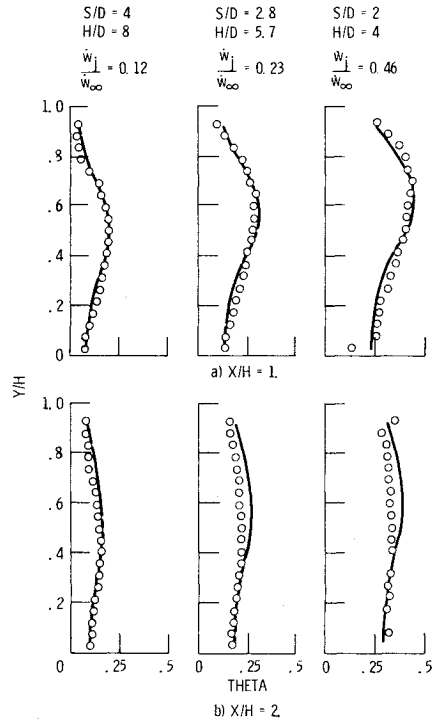

Fig. 11 Effect of varying orifice diameter on centerplane temperature profiles at constant S/H; $S/H = .5$, $J = 25$.

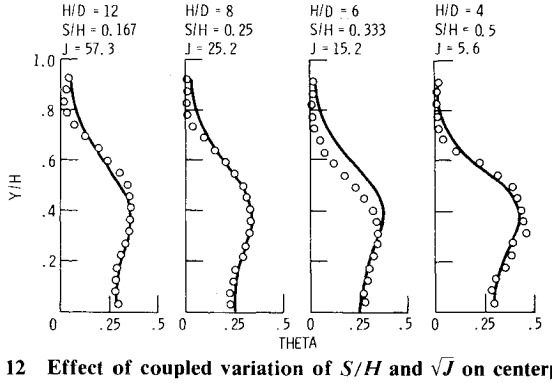

Fig. 12 Effect of coupled variation of S/H and $\sqrt{J}$ on centerplane temperature profiles at constant $\dot{w}_j/\dot{w}_\infty$; $\dot{w}_j/\dot{w}_\infty = 0.23$, $S/D = 2$, $X/H = 1$.

shape of the temperature profiles is not altered appreciably. This effect is shown by the predicted and experimental centerplane profiles at $X/H = 1$ and 2 in Fig. 11 for three orifice configurations with a constant $S/H = 0.5$, but with jet flow-to-mainstream flow ratios varying from 0.12 to 0.46. The profiles shown in Figs. 8, 9, and 11 suggest that for $J = 25$, optimum mixing of the jets with the mainstream flow is achieved with $S/H = 0.5$. The profiles in Fig. 7 show that for $J = 6$, the best mixing was achieved with $S/H = 1$, and for $J = 60$, the best mixing was achieved with $S/H = 0.25$.

The coupling between the momentum flux ratio and S/H is shown further by the centerplane profiles at $X/H = 1$ in Fig. 12. Here the ratio of jet flow to mainstream flow is held constant ($\dot{w}_j/\dot{w}_\infty = 0.23$), and a nearly constant product of $\sqrt{J}$ and S/H is maintained. This coupling gives very similar temperature distributions. It is interesting to compare these profiles, where $\dot{w}_j/\dot{w}_\infty$ is constant, to those in Fig. 9, where J is constant.

Application to Combustor Design

These results suggest that for a given momentum flux ratio and downstream distance, combustor design procedure should first identify the S/H value required to obtain the desired profile shape, and to position the profile at the desired spanwise location. The orifice size would then be chosen to provide the required jet-to-mainstream flow ratio. Because the penetration varies slightly with orifice size, adjustments (using the correlation relations in the flow model) would be necessary to arrive at the final dilution jet configuration. Although the geometries and test conditions of the experimental data base are representative of current desing practice for annular gas turbine combustors, the flow model cannot completely describe dilution zone performance, since, as discussed by Cox,[4] the effects of liner cooling airflow, nonuniform dilution zone inlet temperature distribution, and flow area convergence in the dilution zone are not considered. Also, the experiments were for jets injected from one side toward an opposite wall, thus the results are applicable to one-side entry combustors or (since the wall may be considered to be a plane of symmetry as shown by the opposed jet and jet/wall data in Ref. 6) to dual-side entry combustors with directly opposed jets. At present there are no experimental data available that could be used to extend the model to dual-side, staggered-jet dilution configurations.

Table 1 Standard deviation of correlations

Parameter	Equation	σ
$Y_{c,o}/D_j$	A2	0.752
$\theta_{c,o}$	A3	0.036
$\theta^{+}_{\min,o}/\theta_{c,o}$	A4	0.122
$\theta^{-}_{\min,o}/\theta_{c,o}$	A5	0.734
$W^{+}_{1/2,o}/D_j$	A6	0.660
$W^{-}_{1/2,o}/D_j$	A7	0.550
$Y_{c,z}/Y_{c,o}$	A8	0.121
$\theta_{c,z}/\theta_{c,o}$	A9	0.111
$\theta^{\pm}_{\min,z}/\theta_{c,z}$	A10	....[a]
$W^{\pm}_{1/2,z}/D_j$	A11	....[a]

[a] Standard deviation not available.

Summary of Results

An empirical model is presented for predicting the temperature distribution downstream of a row of dilution jets injected normal to a hot confined crossflow. The model is based on the assumption that all properly nondimensionalized vertical temperature profiles can be expressed in a self-similar form. The scaling parameters in this form have been correlated in terms of the independent variables. These are the momentum flux ratio ($6 < J < 60$), the ratio of the spacing between adjacent orifices to the orifice diameter ($2 < S/D < 6$), the ratio of the duct height to the orifice diameter ($4 < H/D < 16$), the dimensionless downstream distance ($0.25 < X/H < 2$), and the dimensionless off-centerplane distance ($0 < Z/S < 0.5$). Profiles predicted using the flow model are in excellent agreement with the experimental data except for combinations of the flow and geometric variables which result in strong impingement on the opposite wall.

The effects of parametric variation of the independent variables on the predicted and experimental profiles can be summarized as follows:

1) The momentum flux ratio was the most important independent flow variable influencing the penetrations and mixing. For the limited range of density ratios covered by the experiments, no correlation with density ratio was found.

2) For a given orifice diameter, increasing the spacing between adjacent jets increased the penetration and increased the uniformity of the vertical profiles. However, horizontal distributions became more nonuniform with increased spacing as the mixing became more three dimensional.

3) For a constant spacing to diameter ratio (S/D), penetration and mixing at any X/H increased with increasing jet diameter.

4) For a constant spacing (S/H), increasing the orifice diameter increased the magnitude of the temperature dif-

ference ratios, and increased the penetration slightly, but the basic shape of the profiles was not altered appreciably.

Appendix – Correlations

The temperature difference ratio, θ, at any point in the flowfield is determined from:

$$\theta=\theta^{\pm}_{\min}+(\theta_c-\theta^{\pm}_{\min})\exp\left[-\ell n\ 2\left(\frac{Y-Y_c}{W^{\pm}_{1/2}}\right)^2\right] \tag{A1}$$

The correlations for the scaling parameters in this expression are given by equations (A2) to A(11), with the standard deviation, σ, for each correlation given in Table 1. A second subscript has been appended to each of the parameters to denote the transverse location (from $Z=0$ (centerline) to $Z=S/2$ (midplane)) for which the expression is appropriate. The length scales Y_c and $W^{\pm}_{1/2}$, are nondimensionalized using the jet diameter D_j where $D_j=D\sqrt{C_d}$, and $0.62<C_d<0.66$. The primary dimensionless independent variables are J, S/D_j, H/D_j, and X/D_j. In some of the expresions other combinations are used to provide a better insight into the physically important variables or to reduce the number of independent variables needed.

Correlations for Predicting the Centerplane Temperature Profiles

Thermal Trajectory (Centerline)

$$\frac{Y_{c,o}}{D_j}=0.539\,J^{0.25}\left(\frac{S}{D_j}\right)^{0.14}\left(\frac{H}{D_j}\right)^{0.38}\left(\frac{X}{D_j}\right)^{0.17}e^{-b} \tag{A2}$$

where

$$b=\left[0.091\left(\frac{X}{H}\right)^2\left(\frac{H}{S}-\frac{\sqrt{J}}{3.5}\right)\right]$$

The exponential term in this expression is required to suppress the predicted penetration when the main flow is blocked by the establishment of a two-dimensional wall jet flow.

Centerline Temperature Difference Ratio

$$\theta_{c,o}=\theta_{EB}+(1-\theta_{EB})\left[1.452\,J^{-0.35}\Big/\left(\frac{X}{D_j}\right)\right]^f \tag{A3}$$

where

$$f=1.15\sqrt{\frac{S}{H}\Big/\left(1+\frac{S}{H}\right)}$$

and

$$\theta_{EB}=\frac{\dot{w}_j/\dot{w}_\infty}{1+\dot{w}_j/\dot{w}_\infty}$$

θ_{EB} is the temperature difference ratio which would result from complete mixing of the jet and mainstream flows, and thus represents the asymptotic condition for the $\theta_{c,o}$ decay. The decay exponent f varies from 0.38 to 0.81 for the conditions tested in this study. The data of Ref. 6, which were for heated jets in a confined crossflow show a similar $\theta_{c,o}$ decay characteristic. In Ref. 7, a decay exponent of 0.63 was found appropriate for a single jet injected perpendicular to a semi-infinite crossflow. For a round jet in a coflowing stream, an exponent of 0.67 would be expected.

Minimum Centerplane Temperature Difference Ratios

$$\frac{\theta^{+}_{\min,o}}{\theta_{c,o}}=1-e^{-c^+} \tag{A4}$$

where

$$c^+=0.038\,J^{1.62}\left(\frac{S}{D_j}\right)^{1.5}\left(\frac{H}{D_j}\right)^{-3.67}\left(\frac{X}{D_j}\right)^{1.1}$$

$$\frac{\theta^{-}_{\min,o}}{\theta_{c,o}}=1-e^{-c^-} \tag{A5}$$

where

$$c^-=1.57\,J^{-0.3}\left(\frac{S}{D_j}\right)^{-1.4}\left(\frac{X}{D_j}\right)^{0.9}$$

Centerplane Half-Widths

$$\frac{W^{+}_{1/2,o}}{D_j}=0.162\,J^{0.18}\left(\frac{S}{D_j}\right)^{-0.25}\left(\frac{H}{D_j}\right)^{0.5}\left(\frac{X}{D_j}\right)^{0.5} \tag{A6}$$

$$\frac{W^{-}_{1/2,o}}{D_j}=0.20\,J^{0.15}\left(\frac{S}{D_j}\right)^{0.27}\left(\frac{H}{D_j}\right)^{0.5}\left(\frac{X}{D_j}\right)^{0.12} \tag{A7}$$

Note that in this investigation the jet half-widths are defined as the vertical distance from the centerline to where $\theta=(\theta_{c,o}+\theta^{+}_{\min,o})/2$.

Caution should be exercised in comparing the apparent profile widths directly with the half-width correlation relations, since the apparent widths of the profiles depend on $\theta_{c,o}$ and $\theta^{\pm}_{\min,o}/\theta_{c,o}$ in addition to $W^{\pm}_{1/2,o}/D_j$.

Correlations for Predicting the Off-Centerplane Variation of the Temperature Profile Scaling Parameters

Off-Centerplane Penetration

$$\frac{Y_{c,z}}{Y_{c,o}}=1-\left(\frac{Z}{S/2}\right)^2e^{-g} \tag{A8}$$

where

$$g=0.227\,J^{0+67}\left(\frac{S}{D_j}\right)^{-1}\left(\frac{X}{D_j}\right)^{0.54}$$

Off-Centerplane Maximum Temperature Difference Ratio

$$\frac{\theta_{c,z}}{\theta_{c,o}}=1-\left(\frac{Z}{S/2}\right)^2e^{-d} \tag{A9}$$

where

$$d=0.452\,J^{0.53}\left(\frac{S}{D_j}\right)^{-1.53}\left(\frac{X}{D_j}\right)^{0.83}$$

Note that in this investigation the jet half-widths are defined as the vertical distance from the centerline to where $\theta=(\theta_{c,o}+\theta^{\pm}_{\min,o})/2$.

$$g=0.227\,J^{0.67}\left(\frac{S}{D_j}\right)^{-1}\left(\frac{X}{D_j}\right)^{0.54}$$

In Eqs. (A8) and (A9), the ratios of midplane to centerplane penetration and temperature difference are obtained at $Z=S/2$. The exponents g and d in these expressions were derived by correlating the midplane data. The parabolic form was chosen for the centerplane to midplane variation because of its simplicity, and because it gives $d\theta_c/dz=0$ and $dY_c/dz=0$ at the centerplane as required by symmetry.

Off-Centerplane Minimum Temperature Difference Ratios and Half-Widths

$$\frac{\theta^{\pm}_{\min,z}}{\theta_{c,z}}=\frac{\theta^{\pm}_{\min,o}}{\theta_{c,o}} \tag{A10}$$

$$\frac{W^{\pm}_{1/2,z}}{D_j} = \frac{W^{\pm}_{1/2,o}}{D_j} \quad \text{(A11)}$$

No estimate of the standard error is available for Eqs. (A10) and (A11). These relations represent major simplifying assumptions and are justified by the agreement between predicted and experimental off-centerplane profiles shown here and in Ref. 3.

References

[1]Holdeman, J. D., Walker, R. E., and Kors, D. L., "Mixing of Multiple Dilution Jets with a Hot Primary Airstream for Gas Turbine Combustors," AIAA Paper 73-1249, Las Vegas, Nev., 1973.

[2]Walker, R. E. and Kors, D. L., "Multiple Jet Study," June 1973, Aerojet Liquid Rocket Co., Sacramento, Calif.; also NASA CR-121217, 1973.

[3]Walker, R. E. and Eberhardt, R. G., "Multiple Jet Study Data Correlations," April 1975, Aerojet Liquid Rocket Co., Sacramento, Calif.; also NASA CR-134795, 1975.

[4]Cox, G. B., Jr., "Multiple Jet Correlations for Gas Turbine Engine Combustor Design," ASME Paper 75-GT-45, Houston, Tex., 1975.

[5]Norgren, C. T. and Humenik, F. M., "Dilution Jet Mixing Study for Gas-Turbine Combustors," NASA TN D-4695, Aug. 1968.

[6]Kamotani, Y. and Greber, I., "Experiments on Confined Turbulent Jets in Cross Flow," NASA CR-2392, March 1974.

[7]Holdeman, J. D., "Correlations for Temperature Profiles in the Plane of Symmetry Downstream of a Jet Injected Normal to a Crossflow," NASA TN D-6966, Sept. 1972.